

Kinetically driven helix formation during the homopolymer collapse process

Sid Ahmed Sabeur,¹ Fatima Hamdache,¹ and Friederike Schmid²

¹ *Département de Physique, Faculté des Sciences, USTO, Oran 31000, Algeria*

² *Fakultät für Physik, Universität Bielefeld, D - 33615 Bielefeld, Germany*

(Dated: November 19, 2018)

Using Langevin simulations, we find that simple 'generic' bead-and-spring homopolymer chains in a sufficiently bad solvent spontaneously develop helical order during the process of collapsing from an initially stretched conformation. The helix formation is initiated by the unstable modes of the straight chain, which drive the system towards a long-lived metastable transient state. The effect is most pronounced if hydrodynamic interactions are screened.

PACS numbers: 36.20.Ey, 82.37.-j, 87.15.He

Helices are among the most common structures in nature. They are simple shapes which can be stabilized rather easily with suitable potentials [1, 2, 3]. α -helices in proteins have the favorable property of being highly "designable" in the sense that they are robust to mutations and thermodynamically stable [4]. Hence helices are interesting structures from a static point of view. In this Rapid Communication, we report on a dynamic nonequilibrium phenomenon where they also appear spontaneously, for purely kinetic reasons, without special potentials or local constraints [5]: In computer simulations, we find that simple, "generic" polymers in suitable environments recoil into well-ordered helices when released from an initially stretched configuration. This happens despite the fact that the ground state of the polymers is definitely non-helical. The helices emerge as metastable transient states with a finite, temperature-dependent lifetime, which may become quite large.

The dynamics of polymer collapse has been studied in generic model chains by a number of authors [6, 7, 8, 9]. Our work differs from these studies in two aspects. First, we study quenches to very low temperatures, about 1/100 of the Theta temperature. Second, we do not start from an equilibrated high-temperature conformation (a coil), but from a stretched chain. Hence we study "mechanical" quenches rather than temperature quenches. Such rapid mechanical quenches are realized, *e.g.*, if the chain is attached at both ends to objects that move apart, by links that are weak enough that they eventually break up.

We have observed helix formation for various different choices of potentials. In this Rapid Communication, we restrict ourselves to the simple case of Lennard-Jones beads connected by harmonic springs for clarity of presentation. Beads that are not direct neighbors on the chain interact *via* a truncated Lennard-Jones potential

$$V_{LJ}(r) = \begin{cases} 4\epsilon[(\sigma/r)^{12} - (\sigma/r)^6 + c_0] & \text{for } r < 2.5\sigma \\ 0 & \text{otherwise,} \end{cases} \quad (1)$$

where the constant c_0 is chosen such that the potential is continuous everywhere. Adjacent beads in the chain are

connected by bonds subject to the spring potential

$$V_{\text{bond}}(r) = a(r - r_0)^2 \quad (2)$$

with $a = 100\epsilon/\sigma^2$ and $r_0 = 0.85\sigma$. The theta temperature for these chains is of the order $k_B T_\theta \sim \epsilon$ [10]. We investigate the kinetics of chain collapse at temperatures that are 10-100 times lower, starting from an initially straight chain. As dynamical model for the motion of the beads we use Langevin dynamics with and without hydrodynamics. Inertia effects are taken to be negligible [11]. The natural units of our simulation are defined in terms of the bead size σ , the Lennard-Jones energy ϵ , and the friction coefficient ζ (see below). Based on these quantities, the time unit is $\tau = \zeta\sigma^2/\epsilon$.

We begin with discussing the collapse dynamics without hydrodynamics. The solvent surrounding the chain is then effectively replaced by the friction ζ and a Gaussian distributed stochastic force $\vec{\eta}_i$ acting on the monomer i , which fulfills the conditions [12] $\langle \vec{\eta}_i \rangle = 0$ and

$$\langle \eta_{i,\alpha}(t)\eta_{j,\beta}(t') \rangle = 2\zeta k_B T \delta_{ij}\delta_{\alpha\beta} \delta(t - t'), \quad (3)$$

with monomer indices $i, j = 1 \dots N$, cartesian directions $\alpha, \beta \in \{x, y, z\}$, and t, t' two given times. The equations of motion are

$$\zeta \dot{\vec{r}}_i = \vec{f}_i + \vec{\eta}_i. \quad (4)$$

They are integrated using an Euler algorithm with the time step $\Delta_t = 5 \times 10^{-4}\tau$. The stochastic noise $\vec{\eta}_i$ was implemented by picking random numbers with uniform distribution, but the correct mean and variance (3) at every time step [13].

Figure. 1 shows examples of a collapsing chain at moderate and very low temperature ($T = 0.5\epsilon/k_B$ and $T = 0.01\epsilon/k_B$, respectively). At moderate temperature, a variant of the well-known pearl-necklace scenario [6, 7] is recovered: The collapse starts with the formation of small globules at both ends of the chain, which subsequently grow in size and finally merge into a single globule. At low temperature, the scenario is entirely different: Instead of disordered globules, well-ordered helices appear at the ends of the chain. This process is symmetry-breaking, since the model potentials do not impose any

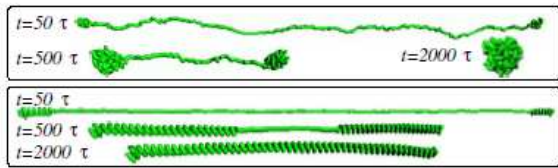


FIG. 1: Configurations of an initially stretched chain with length $N = 200$ monomers at different times t for the temperature $T = 0.5\epsilon/k_B$ (top) and $T = 0.01\epsilon/k_B$ (bottom).

chirality. The helical structures then propagate along the chain, until they meet in the middle. The final chain structure is an almost perfect helix with possibly one defect in the middle, depending on whether the chiralities of the two merging helices match each other. It is characterized by the radius $R \sim 0.5\sigma$, the pitch $D \sim 1\sigma$, and has roughly $n \sim 4$ monomers per turn.

Simple energy considerations show that these helices are by no means the ground state of the chain. The lowest energy state of an infinitely long chain, where surface effects can be neglected, is most likely a structure with close-packed parallel strands. A straightforward energy minimization for this structure yields the energy per monomer $U_{tot}/N = -7.75\epsilon$. In contrast, the lowest possible energy per monomer of an infinitely long helix is $U_{tot}/N = -3.26\epsilon$, which is clearly higher. This is of course not surprising, given that helices have a large, energetically unfavorable polymer-solvent interface. They cannot possibly be ground states at infinite chain length. The question remains whether the finitely long chains considered in the simulations have a helical ground state. The exact calculation of the ground state energy for chains of finite length is a formidable task. We have estimated an upper bound with the method of simulated annealing. At chain length $N = 50$, we get $U_{tot} < -210\epsilon$, corresponding to $U_{tot}/N < -4.2\epsilon$ per monomer, which is well below the energy of an optimized helix. The low energy conformations do not even exhibit local helical order. Hence we conclude that chains of length $N = 50$ or longer are not helical: The helical state observed in the simulations is a kinetic trap.

Intriguingly, it does not even correspond to the energetically optimized helix. The energy minimization for helical structures (minimized with respect to the radius, the pitch, and the bond length) yields a series of local minima characterized by different numbers n of monomers per turn, *i.e.*, $n = 3.92, 4.81, 5.75, 6.71, \dots$. The lowest minimum is at $n = 4.81$. The structures of the helices shown in Fig. 1 are closer to the structure corresponding to $n = 3.92$ with an energy per monomer $U_{tot}/N = -3.04\epsilon$.

Insight into the initial process of helix formation can be gained from a linear stability analysis of the starting conformation, the stretched chain. The unperturbed reference state is an energetically relaxed straight chain with

bond length $b \approx b_0$. The Eigenmodes of the Hessian matrix are the longitudinal (L) and transverse (T) phonons of this chain. Neglecting chain end effects, they have the wavelengths $\lambda_m = bN/m$ and the frequencies [14]

$$\omega_{m,L}^2 = a + \frac{d^2V_{LJ}}{dr^2} (\cos(2\pi b/\lambda_m) + 1) \quad (5)$$

$$\omega_{m,T}^2 = \frac{dV_{LJ}}{dr} \frac{1}{2b} (\cos(2\pi b/\lambda_m) - 1), \quad (6)$$

where d^2V_{LJ}/dr^2 is negative and dV_{LJ}/dr is positive. Unstable modes are characterized by imaginary frequencies. If the spring constant a is sufficiently large, the straight chain conformation is stable with respect to all longitudinal phonons. However, it is unstable with respect to transverse phonons with short wavelengths, $\lambda < 4b$. Hence helical modes with less than $n = 4$ beads per turn are unstable. The most unstable phonon mode corresponds to a zigzag mode. Indeed, weak zigzags are observed at the onset of the collapse process, but helix formation soon takes over, due to the fact that the helical state corresponds to a local energy minimum. We conclude that the helix formation is initially a driven process. This explains why the system picks the helical state with $n = 3.92$, rather than the optimized helical state at $n = 4.81$.

The subsequent collapse is analyzed most conveniently in a slightly modified system where one chain end is fixed, corresponding, *e.g.*, to a grafted chain. The helix formation then proceeds from only one end (the free end), and the defect in the middle of the chain is avoided. Following Kemp and Chen [15], we define the two helical order parameters

$$H_4 = \left(\frac{1}{N-2} \sum_{i=2}^{N-1} \hat{u}_i \right)^2, \quad H_2 = \frac{1}{N-3} \sum_{i=2}^{N-2} \hat{u}_i \cdot \hat{u}_{i+1}. \quad (7)$$

where the \hat{u}_i are unit vectors proportional to $\vec{u}_i \propto (\mathbf{r}_i - \mathbf{r}_{i-1}) \times (\mathbf{r}_{i+1} - \mathbf{r}_i)$, and N is the chain length. The parameter H_4 characterizes the global helical order, and H_2 the local order along the chain.

Fig. 2a) shows a typical time evolution of the order parameter H_4 for such a chain at the temperature $T = 0.04\epsilon/k_B$. One can distinguish two stages: In the beginning, H_4 rises linearly up to a saturation value. This corresponds to a driven regime, where first the instability described above triggers the formation of a helix at the free chain end, and then this helix propagates into the chain. In the second stage, the chain stays perfectly helical for a while, until suddenly part of the helical order gets lost. To analyze this second stage, we have recorded the lifetimes of the helical state in 200 independent runs (different random numbers), starting from an identical helical chain conformation. The lifetime was defined as the time when the energy dropped below a given threshold E_t , which was chosen below the initial energy E_0 such that $E_0 - E_t$ was of the order 1ϵ , much larger than

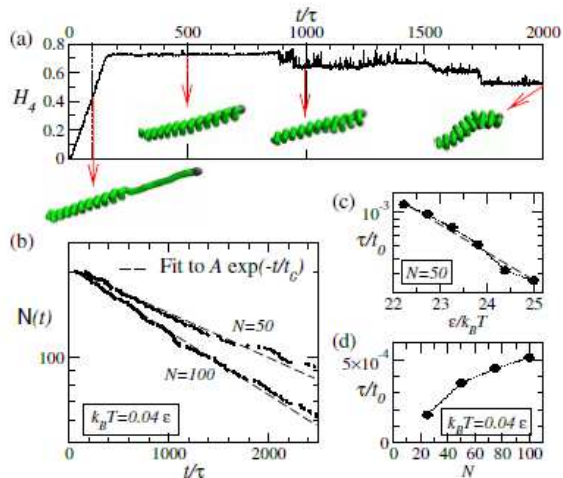


FIG. 2: Time evolution of helical order for endgrafted chains with length $N = 50$ at temperatures around $k_B T/\epsilon \sim 0.04$. (a) Evolution of order parameter H_4 for one specific run, with corresponding chain conformations (grafting point is represented by a dark sphere). (b) Number $N(t)$ of remaining purely helical conformations after the time t in a sample of 200 initially helical conformations, at temperature $k_B T/\epsilon = 0.04$ for two chain lengths as indicated. Dashed lines show fits to an exponential, $N(t) \sim \exp(-t/t_0)$ with escape time t_0 . (c,d) Escape rates $1/t_0$ in units of $1/\tau$ as a function of chain length for the temperature $k_B T/\epsilon = 0.04$ (c), and as a function of the inverse temperature for the chain length $N = 50$ (d). Dashed line in (c) shows the result of a fit to $1/t_0 \propto \exp(-\Delta E/k_B T)$, giving $\Delta E = 0.041 \pm 0.002\epsilon$.

the typical energy fluctuations of an intact helix (roughly 0.002ϵ per monomer). To ensure that the results did not depend on the threshold, we carried out the analysis for at least two different threshold values that differed by 1ϵ , and checked that the results did not change. This was done for a range of chain lengths, $N = 25 - 100$, and temperatures, $k_B T/\epsilon = 0.04 - 0.045$. In all cases, the distribution of the lifetimes was nicely exponential. Two examples are shown in Fig. 2b). We conclude that the decay from the “perfect” helical state is a stochastic, rate-driven process. According to Kramer’s rate theory [16], the height of the energy barrier, ΔE , can be estimated from the temperature dependence of the escape rate, $1/t_0 \propto \exp(\Delta E/k_B T)$. The fit of our data to this law gives $\Delta E = 0.041\epsilon$ (Fig. 2c). Hence perfect helices should persist for a long time at temperatures well below $\Delta E/k_B$, and decay rapidly at temperatures above $\Delta E/k_B$. This is indeed observed in the simulations.

More insight into the nature of the escape process can be gained from looking at the dependence of the escape rate $1/t_0$ on the chain length N . We assume that the escape is initiated by the nucleation of some defect. If this defect is localized at the end of the chain, $1/t_0$ should not depend on N ; if it is localized somewhere in the middle, $1/t_0$ should be proportional to N . Fig. 3d) shows that

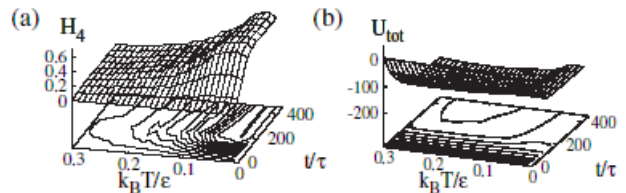


FIG. 3: Time evolution of the helical order parameter H_4 (a) and the total energy U_{tot} (b) in units of ϵ at temperatures between $k_B T/\epsilon = 0$ and $k_B T/\epsilon = 0.3$ for initially stretched chains, averaged over 180 independent runs. The distance between levels in the contour plots is 0.05 in (a) (lowest level 0.05) and 20ϵ in (b) (lowest level -180ϵ).

the escape rate increases with N , thus the escape defect forms in the middle of the chain rather than at the end. However, the dependence is not strictly linear; the true situation is more complicated than our simple argument suggests.

At temperatures above $T = 0.04\epsilon/k_B$, the “perfect” helices decay rapidly, but the system still retains helical order. To determine the temperature range where long-lived helices appear, be they perfect or imperfect, we have calculated the average time evolution of H_4 for temperatures up to $T = 0.3\epsilon/k_B$. The result is shown in Fig. 3a). Helices are observed at temperatures up to $T \sim 0.1 - 0.15\epsilon/k_B$. It is worth noting that in this helical regime, the average total energy U_{tot} is higher than at higher temperatures (Fig. 3b)). This proves once more that the helical state does not correspond to a true free energy minimum [17].

Up to now, hydrodynamic effects mediated by the solvent were disregarded. To assess the influence of the latter, we have also carried out simulations of a dynamical model that includes hydrodynamic interactions *via* an appropriate mobility tensor D_{ij} . Eq. (4) is then replaced by [18]

$$\dot{\vec{r}}_i = \sum_j D_{ij} \vec{f}_j + \sum_j \xi_{ij} \vec{\eta}_j, \quad (8)$$

where $\vec{\eta}$ is distributed as before (Eq. (3)) and ξ fulfills $\xi \xi^T = D$. When determining the mobility tensor for our chains, we must account for the fact that they are endgrafted: The first bead is subject to a constraint force that ensures $\vec{v}_1 \equiv 0$ in Eq. (8). In the absence of noise, the total force on bead 1 is thus given by $\vec{f}_1 = -\sum_{j \neq 1} [D_{11}^{\text{free}}]^{-1} D_{1j}^{\text{free}} \vec{f}_j$, where D_{ij}^{free} is the mobility tensor for free chains. Hence the effective mobility matrix between the remaining beads is

$$D_{ij} = D_{ij}^{\text{free}} - D_{i1}^{\text{free}} [D_{11}^{\text{free}}]^{-1} D_{1j}^{\text{free}}. \quad (9)$$

The free mobility tensor D^{free} was approximated by the Rotne-Prager tensor [18, 19] with solvent viscosity ζ . The ‘square root’ tensor ξ was determined by means of a Cholesky decomposition of D .

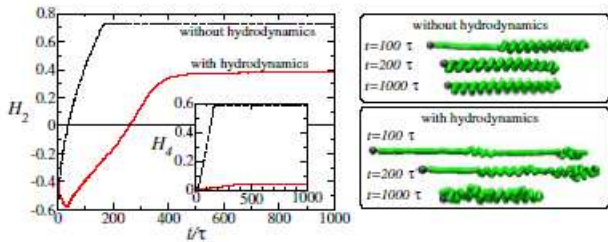


FIG. 4: Left: Time evolution of the local helical order parameter H_2 (main plot) and the global order parameter H_4 (inset) in an initially stretched chain of length $N = 50$ at temperature $k_B T = 0.01\epsilon$ without (dashed lines) and with (straight lines) hydrodynamic interactions, averaged over 100 samples. Right: Examples of corresponding conformations.

Fig. 4 shows the average time evolution of the helical order in such a chain at $T = 0.01\epsilon/k_B$. At this temperature, simple Langevin motion yields highly ordered long-lived helices (cf. Fig. 1). In the presence of hydrodynamic interactions, the overall motion of the chain is much more cooperative, and the local propagation mechanism for helices does not work. As a result, the perfect global helical order disappears, only local order remains. We note in passing that the most unstable chain mode, the zigzag mode, rises to much higher amplitudes and persists much longer in the presence of hydrodynamics than without.

A more detailed account of the hydrodynamic simulations shall be given elsewhere. Here, we just conclude that hydrodynamic interactions largely reduce the effect reported above. The “helical trap” is avoided in the presence of hydrodynamics. This is consistent with previous simulations of chain collapse [8, 9], which also showed that hydrodynamic interactions tend to inhibit trapping during chain collapse.

To summarize, we have observed the spontaneous formation of well-ordered, long-lived helices in Brownian dynamics simulations of simple flexible model polymers at low temperatures. The effect relies on three conditions: (i) The quality of the solvent must be sufficiently bad, *i.e.*, the effective attractive interaction between monomers must be well above the thermal energy $k_B T$. (ii) The chain must be straight initially. The initial conformation then has unstable helical modes, which trigger the helix formation. (iii) Hydrodynamic interactions should be screened. This is the case, *e.g.*, in a porous or molecularly crowded environment. Otherwise, the local ordering process is disturbed by global cooperative processes. Remnant helicity (local helical order) is still observed in the presence of hydrodynamic interactions, but the global order is much reduced.

We speculate that this effect might have contributed to establish helices as one of the most important structural elements in biopolymers. Recently, it has been hypothesized that the early molecular evolution of life may have taken place in strongly confined environments, *e.g.*, thin

interlinked mineral pores [20]. In such environments, hydrodynamic interactions are largely screened, and chains collapsing from stretched conformations may form nicely ordered helices. In an active system where polymers constantly attach and detach to other objects and are permanently stretched and released, helices might thus have appeared perpetually for purely kinetic reasons. They could then have been stabilized *a posteriori* by suitable chemical modifications.

S.A.S. thanks the MHESR, Algeria, and the DFG, Germany (SFB 613) for financial support during an extended visit to Bielefeld. The polymer conformations have been visualized using the open-source package VMD [21].

-
- [1] J.P. Kemp, Z.Y. Chen, Phys. Rev. Lett. **81**, 3880 (1998).
 - [2] D.C. Rapaport, Phys. Rev. E **66**, 011906 (2002).
 - [3] J.R. Banavar, A. Flammini, D. Marenduzzo, A. Maritan, A. Trovato, J. Phys.: Cond. Matt. **15**, S1787 (2003); J.R. Banavar, T.X. Hoang, A. Maritan, F. Seno, A. Trovato, Phys. Rev. E **70**, 041905 (2004).
 - [4] J. Miller, C. Zeng, N. Wingreen, C. Tang, Proteins **47**, 506 (2002).
 - [5] A. Maritan, C. Micheletti, A. Trovato, J.R. Banavar, Nature **406**, 287 (2000).
 - [6] A. Byrne, P. Kiernan, D. Green, K.A. Dawson, J. Chem. Phys. **102**, 573 (1995); Y.A. Kuznetsov, E.G. Timoshenko, K.A. Dawson, J. Chem. Phys. **103**, 4807 (1995); J. Chem. Phys. **104**, 3338 (1996).
 - [7] T. Frisch and A. Verga, Phys. Rev. E **66**, 041807 (2002).
 - [8] R. Chang, A. Yethiraj, J. Chem. Phys. **114**, 7688 (2001); G. Reddy, A. Yethiraj, Macromolecules **39**, 8536 (2006).
 - [9] N. Kikuchi, A. Gent, J.M. Yeomans, Europhys. J. **9**, 63 (2002); N. Kikuchi, J.F. Ryder, C.M. Pooley, J.M. Yeomans, Phys. Rev. E **71**, 061804 (2005).
 - [10] M. P. Taylor, J. Chem. Phys. **114**, 6472 (2001).
 - [11] This is physically reasonable for large (bio)polymers in solution, where the characteristic decay time of the drift velocity of the polymers is usually much smaller (several orders of magnitude) than the time scales characterizing the conformational dynamics.
 - [12] M. Doi, S.F. Edwards, *The theory of polymer dynamics* (Clarendon press, Oxford, 1986).
 - [13] B. Dünweg, W. Paul, Int. J. Mod. Phys. C **2**, 817 (1991).
 - [14] Here, we have made use of the fact that the Lennard-Jones potential is truncated at a distance $r_c < 3b$. The general expression is more complicated.
 - [15] J.P. Kemp and J.Z.Y. Chen, Biomacromolecules **2**, 389 (2001).
 - [16] H. Risken, *The Fokker-Planck equation* (Springer, Berlin, 1989).
 - [17] At thermodynamic equilibrium, the specific heat dU/dT must be positive.
 - [18] D.L. Ermak, J.A. McCammon, J. Chem. Phys. **69**, 1352 (1978).
 - [19] J. Rotne, S. Prager, J. Chem. Phys. **50**, 4831 (1969).
 - [20] P. Baaske, F.M. Weinert, S. Duhr, K.H. Lemke, M.J. Russell, D. Braun, PNAS **104**, 9346 (2007).
 - [21] W. Humphrey, A. Dalke, and K. Schulten, J. Molec. Graphics **14**, 33 (1996).